

Mathematical Approaching and Experimental Assembly to Evaluate the Risks of In-Service Welding in Hot Tapping

Ivo Andrei de O. L Lima

Mem. ASME
Braskem S.A.,
Camaçari 42810-000, Bahia, Brazil
e-mail: ivo.lima@braskem.com

Alex Alisson Bandeira Santos

SENAI CIMATEC—Integrated Center of
Manufacturing and Technology,
Salvador 41650-010, Bahia, Brazil
e-mail: alex.santos@fiob.org.br

The welding onto in-service pipeline (operation condition) results in three possibilities of high risks: leaking and/or explosion by burn-through, chemical reactions to instability, or even explosion due to the heat on internal fluid and cracking in heat affected zone (HAZ). The numerical methods have a useful role in the assessment of welding conditions for the safe in-service welding of pipelines. Only limited published works have considered direct calculation of burn-through using a combination of thermal and stress analysis. The mathematical model of the heat source is the most important part of these numerical models, and actually the mathematical model which described better the heat distribution of the arc welding through gas-shielded tungsten arc welding (GTAW) process or shielded metal arc welding process is the double ellipsoidal heat source (DEHS) model of Goldak and Akhlaghi (2010, Computational Welding Mechanics, Springer Books, New York, pp. 32–35). However, that model has considered the heat source in rectilinear motion only, and it depends on three parameters (a, b, c) which are related with the weld bead size and shape to define the geometry and co-ordinates of heat source, and they are determined empirically or experimentally. Few researchers published works that could determine these parameters mathematically, from the welding data. The publication that best analytically addressed this issue was the work of Eagar and Tsai (1983, “Temperature Fields Produced by Traveling Distributed Heat Sources,” Weld. J., 62(12), pp. 346–355). First, this paper presents a new equation for heat source in double ellipsoid considering the circular motion, trying to develop a model closer to the physical situation of hot tapping onto pipeline. Second, a proposal for determination of the parameters a, b analytically from the Eagar model and Tsai (1983, “Temperature Fields Produced by Traveling Distributed Heat Sources,” Weld. J., 62(12), pp. 346–355), and third, an experimental facility to get the temperature field that was used to validate the numerical finite element models. [DOI: 10.1115/1.4031506]

Keywords: in-service welding, double ellipsoidal heat source, hot tapping, finite element analysis

1 Introduction

The welding onto in-service pipeline (operation condition) results in three possibilities of high risks: leaking and/or explosion by burn-through, chemical reactions to instability, or even explosion due to the heat on internal fluid and cracking in HAZ. According to Sabapathy et al. [1], two factors make in-service welding difficult: the flow of gas (or liquid) creates a large heat loss in the pipe wall, resulting in fast weld cooling. The high strength steels are common in pipelines and are sensitive to high cooling rates that may decrease the toughness of HAZ through formation of hardened areas, increasing the possibility of cracking in the HAZ. The second problem is the loss of mechanical strength due to high temperatures during the welding process with the possibility of localized rupture of the pipe wall due to internal pressure. The rapid cooling can be compensated by increasing the heat input, which in turn causes an increase in the penetration with a consequent increase in the risk of burn-through. The balance between these two factors will establish the safe limits to perform the in-service welding. In addition to these two factors,

there is a third factor that is the interaction between the fluid and the temperature on inner surface of the pipe, which can lead to explosion due to an unstable reaction. This unstable reaction is not treated in almost none references on numerical simulation of welding in-service, but is a reality that must be considered, and is well addressed in API 577 “welding inspection and metallurgy” [2]. The useful role of numerical simulation of welding service has been well demonstrated by the work of EWI/BMI (Edison Welding Institute/Battelle Memorial Institute).

In the industry, one of the most used models to simulate welding/hot tapping in pipeline and piping is the numerical model developed by BMI. This is a 2D model (two-dimensional) finite difference to simulate welding gloves and direct, both to recover corroded pipelines. The model allows to predict the temperature in the inner surface of the pipe and the cooling time of the weld ($\Delta T_{800-500}$), for a given set of welding parameters, geometry and with a coefficient of heat transfer by convection obtained from empirically as a function of the internal fluid. The model determines the risk of penetration (burn-through) indirectly, by applying the “safe” temperature of 980 °C for low hydrogen electrodes and 760 °C for cellulosic electrodes, and it limits the risk of cracking in the HAZ, limiting the hardness to 350 HVN, empirically obtained through the chemical composition of the steel and the $\Delta T_{800-500}$ found. The simulations performed with the numerical

Contributed by the Pressure Vessel and Piping Division of ASME for publication in the JOURNAL OF PRESSURE VESSEL TECHNOLOGY. Manuscript received December 27, 2014; final manuscript received August 28, 2015; published online October 8, 2015. Assoc. Editor: Xian-Kui Zhu.

model of BMI were validated by the EWI, through an experimental method developed by EWI. The model then became known as the BMI/EWI model.

Some limitations in the BMI/EWI model can be observed mainly when the evaluation of the risks is about low thicknesses (<5 mm), they are

- The results were validated by EWI in several tests with thicker pipes (6.35 mm) and medium strength (API 5L-X52). The pipeline industry has advanced strongly to use of higher strength steels (X70, X80) and with thicknesses as low as 3 mm. Under these conditions, the cooling rate increases and the risk of burn-through also. Therefore, some references as well as the codes such as API 2201 "Procedures for Welding or Hot Tapping on Equipment in Service," [3] restrict welding service for thicknesses below 5 mm.
- The limits of 980 °C (low hydrogen electrodes) and 760 °C (cellulosic electrodes) to avoid the risk of penetration (burn-through) are based only on heat input, neglecting the influence of existing thermal stresses or mechanical stresses due to internal pressure. According to Tahami and Asl [4], localized rupture may occur even with partial penetration due to internal pressure and existing thermal stresses.
- The model overestimated the cooling time $\Delta T_{800-500}$ for thinner wall and underestimated for thick-walled pipes. Taking the possibility of selecting heat input (heat inputs) not conservative for pipes of less than 4.8 mm.
- The model is a 2D mesh fixed and the analysis is static. The 2D model does not consider the heat transfer in the longitudinal direction and the static analysis does not consider a multi-layer welding;
- The model considers only a heat source with punctual distribution.

In 1992, Goldak et al. [5] and Sabapathy et al. [6] used a 3D finite element model to calculate the thermal fields for circumferential fillet welds of direct branching. They found that the shape and the weld bead size have a strong influence on the calculated penetration and temperature profile around the weld pool. According to Sabapathy et al. [1], the use of empirical relations between the welding parameters and the size and shape of the weld bead is an appropriate way to define the geometry of the weld and the coordinates of the heat source. Goldak and Akhlaghi [7] developed an equation that characterizes the heat distribution by a nonautogenous welding source, they called it of DEHS, which defines the heat flow Q (kJ/mm³) to a point within the volume defined by ellipsoidal heat source. Figure 1 shows the model and its corresponding equation is shown below:

$$q(x, y, z, t) = \frac{6f\sqrt{3Q}}{abc\pi\sqrt{\pi}} e^{-3x^2/a^2} e^{-3y^2/b^2} e^{-3z^2/c^2} \quad (1)$$

Equation (1) depends on the semi-axes a , b , and c (width, depth, and length) of the weld, and these in turn depend on various factors such as current speed, voltage, arc efficiency, type of

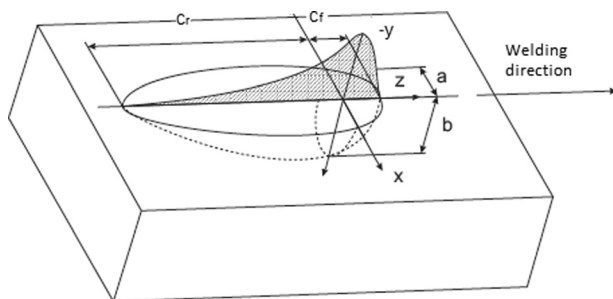


Fig. 1 Model of double ellipsoid of Goldak and Akhlaghi [7]

process, etc. In most cases, the size and shape of the molten weld pool (MZ) can be estimated from data from a metallographic analysis. Since there is no analytical correlation that can determine the parameters a , b and c as a function only of welding variables (voltage, current, etc.), there will always be need to do experimental measurements. For process automation, this approach becomes impractical and expensive, and it will always require building experimental facility to adjust the numerical model. On the other hand, some researchers have developed methods to estimate the size of the MZ and HAZ from welding inputs. The main reference is the method suggested by Christensen et al. [8] has developed a general method for punctual source from the expressions Rosenthal [9]. Besides that, Eagar and Tsai [10] developed a method derived from the work of Christensen et al. [8] for a Gaussian power distribution. However, none of the work presented a method for DEHS distribution until the moment.

For all this, the proposal for a more comprehensive mathematical model is needed, mainly with thickness below 5 mm, it is still a challenge to in-service welding, and with the application of high-strength steels, will become an even greater challenge for the industry, especially oil, gas, and petrochemicals. The doctoral thesis from an author proposes a comprehensive computational model to simulate and evaluate the feasibility of the hot tapping, as the risks related to welding in pipeline and piping, involving its various aspects and parameters with respect to the welding process (amperage, voltage, travel speed, etc.), material properties, characteristics, and operating conditions of the fluid contained in order to prevent burn-through and/or instability chemical reactions of the internal fluid due to heat and/or cracking due to rapid cooling of the HAZ which could result in accident during the welding. For both, the most current solutions numerical modeling were considered, adopted in various reference works cited, but with the distinction of being applied in the same 3D tubular model. Moreover, the work is proposing a new mathematical model for the distribution of heat source in double ellipsoid with circular motion, instead of linear motion, much more adequate the physical situation and an analytical method to determine the parameters a , b , and c from only the welding inputs.

This paper shows the mathematical approaching for a new equation for DEHS with circular motion, an analytical method to determine parameters a , b , and c and the experimental model constructed to evaluate the results from the comprehensive numerical model in finite elements to simulate and evaluate the feasibility of the hot tapping, as the risks related to welding in pipelines.

2 Heat Source Model for Welding

During the process of welding, the heat input melts both the materials added than the base metal around the MZ, from a distinct way than the traditional models with punctual and linear source. The modeling of the heat source is a most important factor to approximate the results of computational models from experimental models.

Figure 2 shows the Gaussian distribution that is more realistic than the punctual distribution and that can be expressed by the equation below:

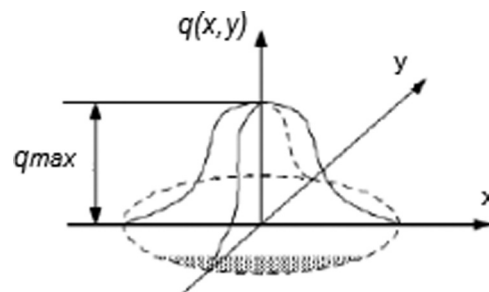


Fig. 2 Gaussian heat source

$$q(r) = q_{\max} \exp(-Cr^2) \quad (2)$$

where $q(r)$ is the surface heat flow at radius r , q_{\max} is the maximum flow of the heat source in the center. C is the concentration coefficient and r is the radial distance from the central source, respectively. The Gaussian distribution can be used for small penetrations processes such as GTAW and SAW (submerged arc welding). However, as it does not reflect the pressure from the arc in the MZ, it is not suitable for welding processes that produce deeper penetration as the electron beam and the laser process. Furthermore, the source model that currently best describes the distribution of heat for welding process by the electric arc is the model of double-ellipsoidal of Goldak and Akhlaghi [7] that describes the three-dimensional distribution of heat to the moving source. Figure 1 shows the model and its corresponding Eq. (1). Where a , b , and c are the semi-axes of the distribution of power density in a Gaussian ellipsoid centered at $(0,0,0)$ and parallel coordinates (x, y, z) . Since Eq. (1) is presented as a function of $\xi = z + v(t - \tau)$ which is movable coordinated proposed by Friedman [11], Krutz and Sergerlind [12] to represent the motion of the source. The parameter a is the width, b is the depth, and c is the length, and c , at downstream of the weld, is the C_f and at upstream is C_r . f is the concentration factor and f at upstream of the weld is f_r and at downstream is f_f . Q is the heat input of welding given by $Q = nVI$, with the arc efficiency n , voltage V , and amperage I .

2.1 New Model—Source With Circular Movement. The expression of Goldak and Akhlaghi [7] was developed for a mobile source in rectilinear direction, distinct from the situation in the joint “T” of the branches made in the hot tapping process. This paper presents a solution for mobile source in cylindrical coordinates to be applied in pipe braches (*hot tapping*). Figure 3 shows the system of Eq. (3) used to describe the circular movement of the weld

$$\left. \begin{aligned} R_{ce} &= \sqrt{x_{ce}^2 + z_{ce}^2} \\ \theta_{sec} &= \sin^{-1} \phi; \theta_{pec} = vt/R_w \\ \phi &= |z/R_{ce}| \end{aligned} \right\} \quad (3)$$

In expression (2), the mobile coordinate ξ describes the rectilinear motion, where v is the linear speed of welding, τ is a delay factor necessary to define the position of the source at the initial time $t = 0$, see Fig. 4(a).

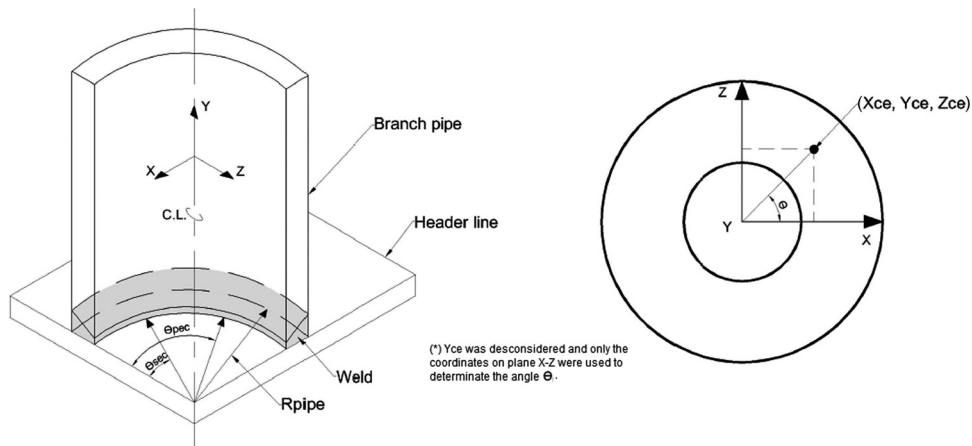


Fig. 3 Cylindrical coordinates for pipe model

In proposed system by this paper, as the movement system is circular, the relative position between the source (θ_{pec}) and position (θ_{sec}) section ahead or behind the source are determined by the difference in angular displacement, see Fig. 4(b). Thus, we must define the factor f as f_r or f_f to set the proper heat distribution in the section. In the finite-element model, the determination of θ_{sec} is done element by element inside each pass and the coordinates (x_{ce}, z_{ce}) are relative to the centroids of the elements.

This paper proposes a new expression for the DEHS due to cylindrical coordinates for a heat source with circular motion according to the equation below:

$$q(R, y, \theta, t) = \frac{6f\sqrt{3}Q}{abc\pi\sqrt{\pi}} e^{-3(x-M)^2/(b|\cos\theta_{pec}|+c|\sin\theta_{pec}|)^2} \times e^{-3(y-t_w)^2/a^2} e^{-3(z-N)^2/(b|\sin\theta_{pec}|+c|\cos\theta_{pec}|)^2} \quad (4)$$

where M is $R_w|\cos\theta_{pec}|$ (note 1) and N is $R_w|\sin\theta_{pec}|$, and they are the coordinates that describe the movement of source as ξ describes the rectilinear motion. θ_i is the starting angle or the beginning of welding. R_w is the radius on gravity center each bead and t_w is the height of gravity center each bead, both relatives to the origin $(0,0,0)$. Note that the parameters a and b are parallel to x and y coordinates, respectively, different from Goldak and Akhlaghi [7] model that represents a butt joint, this model represents a joint T, so with different orientation.

2.2 Knowing the Parameters a , b , and c . Equation (1) depends on the semi-axes a , b , and c (width, depth, and length) of the weld, and these in turn depend on various factors such as current speed, voltage, arc efficiency, type of process, etc. In most cases, the size and shape of the MZ can be estimated from a metallographic analysis. On the other hand, some researchers have developed methods to estimate the size of the MZ and HAZ, and is referred to as the method suggested by Christensen et al. [8] has developed a general method for punctual source from the expressions Rosenthal [9].

In addition, Eagar and Tsai [10] developed a method derived from the work of Christensen et al. [8] for a Gaussian power distribution. This distribution is a good approximation with the GTAW process as mentioned in item 2 above. However, none of the work presented a method for DEHS distribution until the moment.

Note 1: The brackets were used to maintain the absolute values, ensuring the adequate summation and signals, because the mathematical manipulation was developed considering angles at first quadrant from 0 deg to 90 deg.

Two experimental models were constructed to assessment and comparison of the DEHS model by Goldak et al. with the new

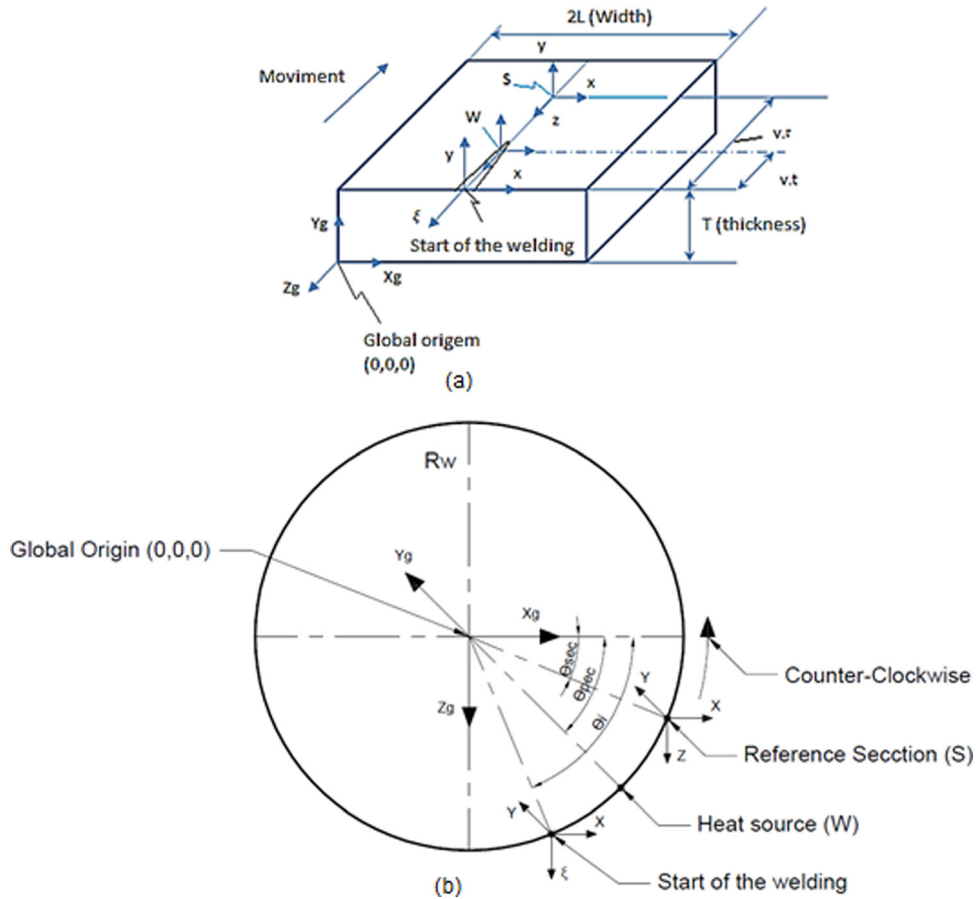


Fig. 4 Coordinate system used for DEHS in rectilinear movement (a) and circular movement (b)

Table 1 Parameters a , b , and c

	Initial values Eagar and Tsai [10]		Experimentally adjusted model 1 linear movement		Experimentally adjusted model 2 circular movement		Mathematical proposal to determine a , b and c See item 2.3			
	Model 1	Model 2	Parameters of heat source (mm) ^a		Parameters of heat source (mm) ^a		Model 1	$\Delta 2^c$	Model 2	$\Delta 2^c$
Parameters of heat source (mm) ^a	A	B	C	[A/C]	D	[B/D]	E	[C/E]	F	[D/F]
a —half width of weld pool	12	6,2	7	1,71	3,8	1,63	6,92	1,01	3,69	1,02
b —depth of weld Pool	8,6	6,0	2,3	3,74	1,26	4,76	2,306	0,97	1,23	1,02
C_f —front source	—	—	14	—	8,2	—	13,84	1,01	7,4	1,1
C_r —rear source	—	—	28	—	16,5	—	27,68	1,01	14,8	1,11

^aThe parameters C_f and C_r were obtained as functions of the parameter a .

^b $\Delta 1$ is (Eagar and Tsai value/experimental value).

^c $\Delta 2$ is (experimental value/mathematically obtained values).

DEHS model proposal made for this work, the first one in linear movement and second one in circular movement. The parameters a , b , and c initially were determined by the method of Eagar and Tsai [10] but they were being adjusted to approximate two numerical models in finite element then the results were compared with experimental measurements. Table 1 presents the initial values obtained by the method of Eagar and Tsai [10] and the final adjusted values on numerical models. Figure 5 shows pictures of the experimental facilities and yours numerical models, respectively.

The numerical simulations were made varying the parameters a and b , until finding out the best combination that resulted in similar values on preselected nodes obtained with the experimental model for the same position of installed thermocouples. Figure 6

shows the position of the installed thermocouples and Figs. 7 and 8 show the results in both models compared with measurements at experimental facilities.

The final adjusted parameters have been divergent when evaluated individually, but they have demonstrated a pattern in proportionality in the same MZ. In model 1 with rectilinear welding, the relationship between the parameters a/b is 3.0, and for the tubular type (model 2) is held at this same proportionality. The values of C_f and C_r are in millimeters and they are consistent with values used in the cited references. In addition, C is the length of the heat source and it is not a transversal dimension of the HAZ or MZ (e.g., width and depth), see Fig. 9.

It is noticed that the parameters a and b are closer to the size of a MZ + HAZ in GTAW process. Moreover, the use of parameters

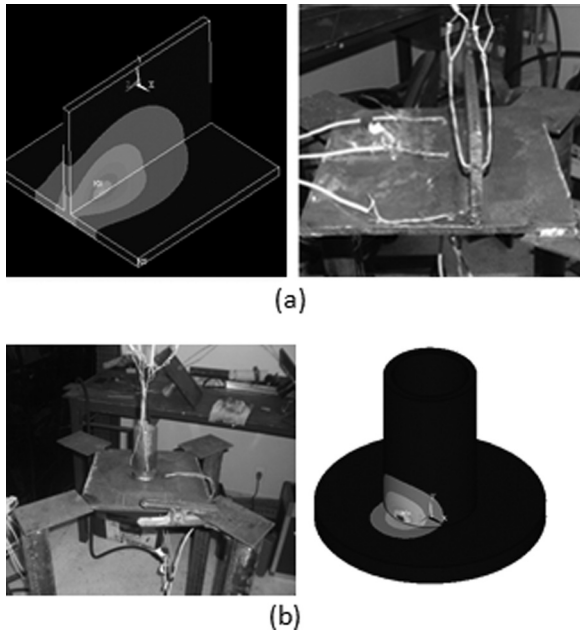


Fig. 5 Experimental models 1 and 2 and your numerical models, respectively

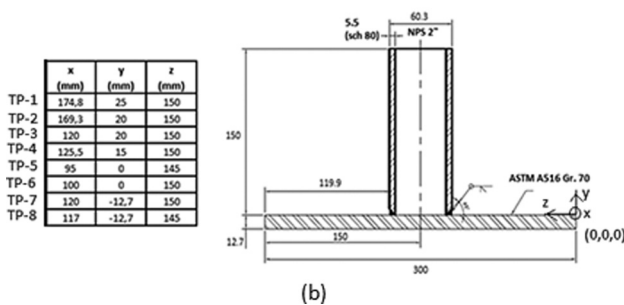
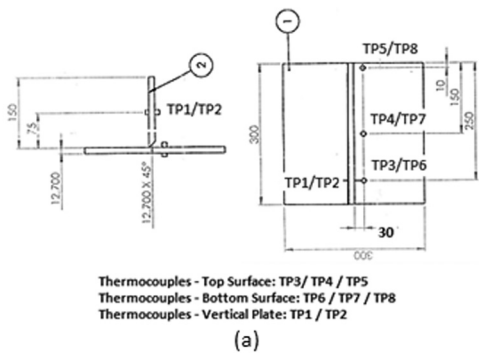


Fig. 6 (a) Plant view and cross section of the model 1, (1) metal base and (2) vertical plate. (b) Plant view and cross section of the model 2.

a and b much closer to the physical dimensions (without prior metallographic measures) resulting in approximated values with the results of the experimental models is one of the major challenges of this type of simulation. The authors believe that there will never a coincidence between the physical measurements and the values of the heat source parameters because there are also other important factors approximated in the numerical models, such as the material properties, arc length, heat input, etc. However, this divergence between the parameters obtained mathematically (e.g., Eagar and Tsai method), the physical dimensions (microscopically measures), and the adjusted values for the numerical models prevents to the generation of a model that

allows the automation of process simulation of in-service welding. Based on the proportionality between the parameters a and b in the results of Table 1, the authors proposed a mathematical method using a system of equations to determine the parameters a , b , and c , and at function of the welding parameters without the need for experimental facilities. Thus making the numerical model proposed by authors complete and which can be used to automate the in-service welding simulation process.

2.3 An Proposal for the Mathematics Determination of the Parameters a , b , and c for DEHS. As can be seen in Table 1, the parameters a and b obtained by Eagar and Tsai method [10] differ from values adjusted to obtain the temperature values in numerical models. However, according to the work's Eagar and Tsai [10], the results obtained with the method are very close for GTAW welding without filler metal, considering a Gaussian distribution. This geometry is reasonable whenever it is a static source, however, in the case of a moving source, the geometry of double ellipsoid has proved to be more efficient. This paper proposed a methodology to determine the parameters a , b , and c for a DEHS distribution, from results of the models by Eagar and Tsai. The fundamental principle of this proposal is that the surface distribution, which is circular in Gaussian, is redistributed taking the ellipsoidal shape during movement. Considering the equivalence between surface areas, as shown in Fig. 10, and knowing the ratio $a/b = 3.0$, the parameters a , b , and c can be determined for DEHS from the values obtained by Eagar and Tsai [10] in the expressions using the below equation:

$$a_e = \frac{2a_g^2}{(c_f + c_r)}; \quad b_e = \frac{a_e}{3} \quad (5)$$

Using the correlation between C_f and C_r recommended by Goldak and Akhlaghi [7] which is $2C_f = C_r$ and using $C_f = 2a$, the parameters a and b can be mathematically determined. Table 1 shows the comparison between the values obtained with Eagar and Tsai, the experimentally adjusted values and the value obtained mathematically by the proposed method.

3 Material and Numerical Modeling

The plates and pipes adopted on experimental facilities were carbon steel, ASTM A 516 gr. 60 and ASTM A 106 Gr. B. The mechanical and thermal properties of material are in accordance with ASME II part D [13] and ASME B31.3 [14], whenever the data are not available in these codes for the required temperature, the properties was obtained from the work of Deng and Murokawa [15]. Table 2 shows the material temperature-dependent properties. The mechanical and thermal properties have been considered as temperature-dependent parameters (nonlinearity).

The 3D-FE (3D finite elements) models have been developed through subroutines in APDL (ANSYS parametric design language) of the finite-element code ANSYS MECHANICAL APDL, release 14.5 [16]. All models were built with solid elements (3D) to consider the thermal and mechanical properties and functions, respectively, in all three directions (x , y , z). Due to the thermomechanical analysis of the solution, coupled-field element type SOLID70 and SOLID185 with eight nodes has been used to create the mesh. These elements allow to perform a coupled physics analysis with the same mesh where the thermal analysis of process is solved independently, and then, using the thermal results, the mechanical stress analysis can be carried out which considers the contributions of the transient temperature fields through thermal expansion. Table 3 shows the main characteristics of the used elements and Fig. 11 shows the finite-element mesh in 1/8 section of the tubular model.

In addition, the physical properties of material have been considered as temperature-dependent parameter, a bi-linear

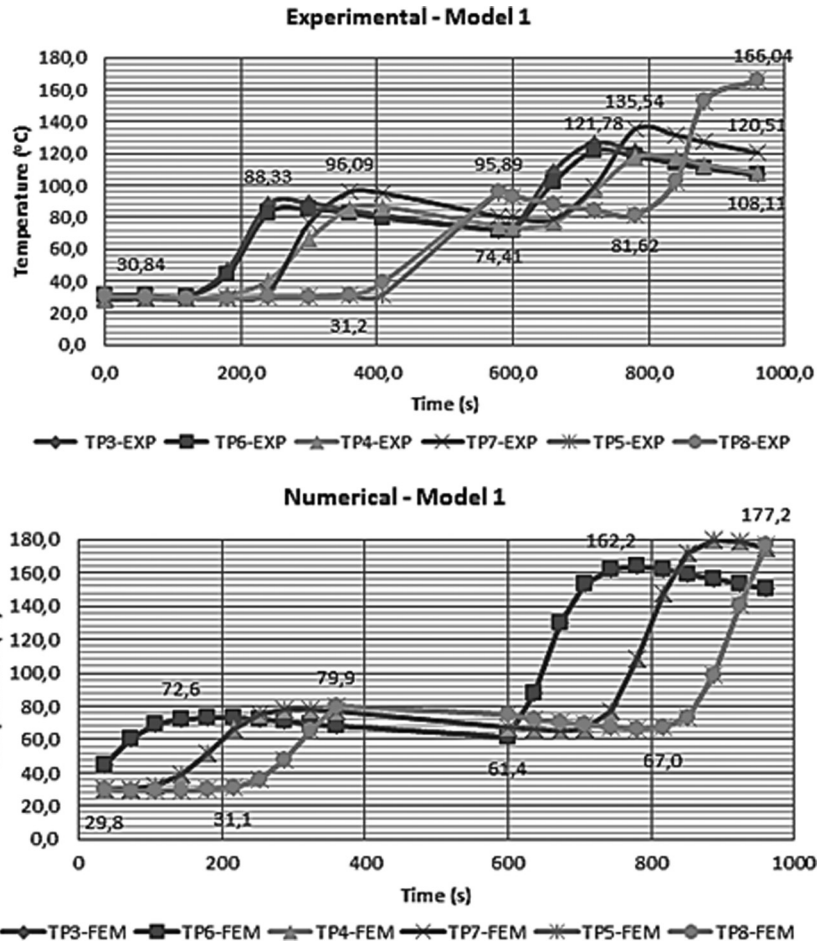


Fig. 7 Experimental and numerical values for the thermocouples TP-3 up to TP-8 during the first and second pass—Model 1

elastoplastic formulation of the material behavior has also been used with the tangent modulus of 4 GPa (see Table 2). The von Mises yield criterion and associated a flow rule is used together with kinematic hardening and the bilinear representation of the stress–strain curve. The addition of filler material (multipass) has been modeled using Element Birth and Death Technique of the ANSYS code with two welding passes (Fig. 11). The Birth and Death Technique modifies the values in the conductivity and stiffness matrixes for the selected then sometimes the elements are turned on and they are turned off in accordance with the subroutine developed in APDL. The addition of each weld pass is modeled by Birth Technique and the heat input is added on individual elements in each weld pass through a distributed heat flux ($W m^{-3}$) established by Eq. (4) and computed by subroutine in APDL. The program uses the full Newton–Raphson procedure, in which the stiffness matrix is updated at every equilibrium iteration. If adaptive descent is on (optional), the program uses the tangent stiffness matrix only as long as the iterations remain stable (i.e., as long as the residual decreases, and no negative main diagonal pivot occurs). If divergent trends are detected on an iteration, the program discards the divergent iteration and restarts the solution, using a weighted combination of the secant and tangent stiffness matrixes. When the iterations return to a convergent pattern, the program resumes using the tangent stiffness matrix. The automatic time stepping has been used.

The generated heat in the welding process will dissipate from the welding zone by radiation, conduction, and convection. The losses by radiation are dominant at higher temperatures and near the MZ and convection losses are dominant at lower temperatures

away from the MZ. To take into account these two factors, a total coefficient of temperature-dependent convection was used [16], as expressions (6).

$$h \left(\frac{W/m^2}{^\circ C} \right) = \begin{cases} 0.0668T & \text{when } 0 \leq T \leq 500^\circ C \\ \text{and } (0.231T - 82.1) & \text{when } T > 500^\circ C \end{cases} \quad (6)$$

where T is the temperature. This boundary condition was applied in all free surfaces as shown in Fig. 12.

4 Experimental Facility to Evaluate the Final Numerical Model

To validate the comprehensive mathematical model proposed by the authors of this work, an experimental facility was built to get the temperature field during in-service welding onto a pressurized tube, approaching the maximum of the real situation to obtain the data. Figure 13(a) shows the general view of the installation where all the equipment and facilities to perform the experimental procedure can be seen. In Fig. 13(b), the major components are indicated numerically.

The experimental assembly is arranged in four main systems: (1) data acquisition system, (2) feed air system, (3) instrumentation, and (4) welding equipment and accessories. Eight thermocouples were used to acquire the temperature values through a data acquisition with the following characteristics:

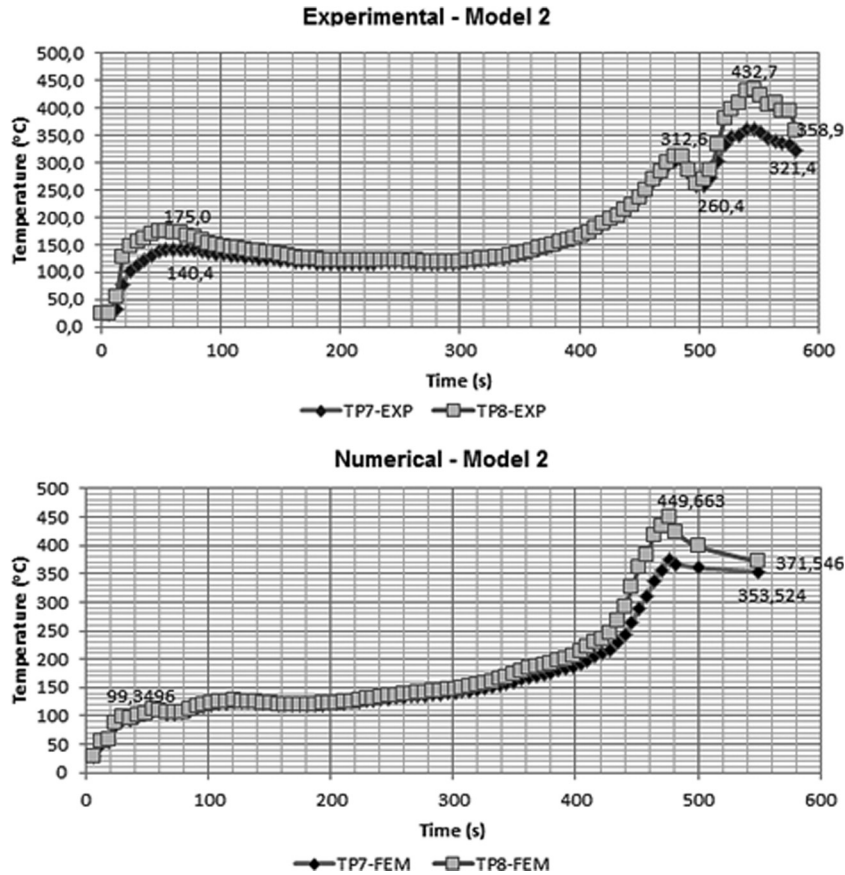


Fig. 8 Experimental and numerical values for the thermocouples TP-7 and TP-8 during the first pass—Model 2

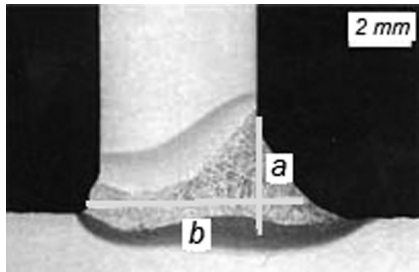


Fig. 9 Width (a) and depth (b) for T joint

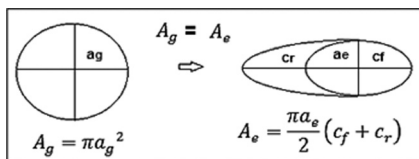


Fig. 10 Equivalence between surface areas

- positive thermal element (KP): Ni90%Cr10% (Cromel)
- negative thermal element (KN): Ni95%Mn2%Si1%Al2% (Alumel)
- application temperature range: -270°C up to 1200°C

- power: -6458 mV up to $48,838\text{ mV}$
- sensibility: $-41\ \mu\text{V}/^{\circ}\text{C}$

The thermocouples type “K” were fixed on the surface of the plates and metal tubes with a connection to resist the heat of welding ($>1200^{\circ}\text{C}$) and maintain a good thermal conductivity, then one capacitive discharge machine was used. Each one of the eight thermocouples was installed in predefined coordinates to compare the measured temperature values with the obtained on nodes in the same position inside the numerical models.

The data acquisition is based on a platform of the National Instruments called Compact Dek, cDAQ-9172 model with NI-9205 module. Measurement uncertainty is established by the manufacturer of the order of 1%. In addition, the temperature, the voltage, and amperage were recorded directly of the power supply. The feeding of the compressed air to the experiment facility is through a screw compressor with gauge pressure up to 0.7 MPa. The operating pressure can be adjusted between 0 and 0.7 MPa by the pressure regulator, LFRD MIDI model from Festo, see item 1 of Fig. 13(b).

The instruments used in the experimental facility to measure temperature, pressure, and flow, which are the parameters required for evaluation of numerical models, are: (1) temperature measurement: thermocouples type K, (2) pressure measurement: manometer, and (3) flow measurement: flowmeter. Items 2, 4, and 8 of Fig. 13(b). The electric arc inert gas (GTAW) was used as the welding process, with the data as shown in Table 4.

The basic parameters to determining the energy of the heat source (Q) are the voltage (V), the amperage (I), and travel speed (v). The two first parameters were collected of the data acquisition, only the travel speed (v) of welding was obtained by dividing

Table 2 Temperature-dependent properties for the carbon steel

Temperature	Conductivity	Diffusivity	Density	Young modulus	Thermal Expansion	Yield stress	Specific heat	Poisson ratio	Tangent modulus
$^{\circ}\text{C}$	K	α	ρ	E	μ	S_y	c	ν	H
$^{\circ}\text{C}$	W/m $^{\circ}\text{C}$	m 2 /h	kg/m 3	MPa	$\mu\text{m/m}/^{\circ}\text{C}$	MPa	J/g $^{\circ}\text{C}$	—	MPa
21	47.2	0.049	7850	2.03×10^5	10.926	220.8	4.40×10^{-1}	0.29	4.00×10^0
93	48.1	0.045	7850	1.99×10^5	11.484	202.17	4.88×10^{-1}	0.295	4.00×10^0
204	45.9	0.040	7850	1.93×10^5	12.276	188.37	5.31×10^{-1}	0.301	4.00×10^0
316	43.1	0.035	7850	1.83×10^5	13.014	169.05	5.70×10^{-1}	0.31	4.00×10^0
427	40.2	0.030	7850	1.67×10^5	13.77	148.35	6.21×10^{-1}	0.318	4.00×10^0
482	38.6	0.027	7850	1.55×10^5	14.112	139.38	6.55×10^{-1}		4.00×10^0
538	36.5	0.024	7850	1.41×10^5	14.346	131.1	6.85×10^{-1}		4.00×10^0
593	34.3	0.022	7850	1.24×10^5	14.616	122.82	7.23×10^{-1}	0.326	4.00×10^0
704	29.2	0.015	7850	8.83×10^4	14.904	106.26	9.20×10^{-1}	0.342	4.00×10^0
760	27.2	0.007	7850	7.04×10^4	15.048	97.98	1.72×10^0		4.00×10^0
816	25.8	0.016	7850	5.24×10^4	15.192	89.7	7.40×10^{-1}	0.35	4.00×10^0
927	29.2	0.020	7850	1.66×10^4	15.48	6.9	6.85×10^{-1}		4.00×10^0
1038	34.3		7850	1.66×10^4	15.768	6.9	7.60×10^{-1}	0.45	4.00×10^0
1204	40.2		7850	1.66×10^4	16.2	6.9	7.72×10^{-1}	0.45	4.00×10^0
1427	45.9	0.027	7850	1.66×10^4	16.776	6.9	7.85×10^{-1}	0.45	4.00×10^0

Table 3 3D solid elements

Element	Main characteristics as defined by ANSYS MECHANICAL APDL 14.5 user's manual
SOLID70	It has a 3D thermal conduction capability. The element has eight nodes with a single degree of freedom, temperature, at each node. The element is applicable to a 3D, steady-state or transient thermal analysis
SOLID185	It is used for 3D modeling of solid structures. It is defined by eight nodes having three degrees of freedom at each node: translations in the nodal x , y , and z directions. The element has plasticity, hyperelasticity, stress stiffening, creep, large deflection, and large strain capabilities. It is the equivalent structural element of the SOLID70

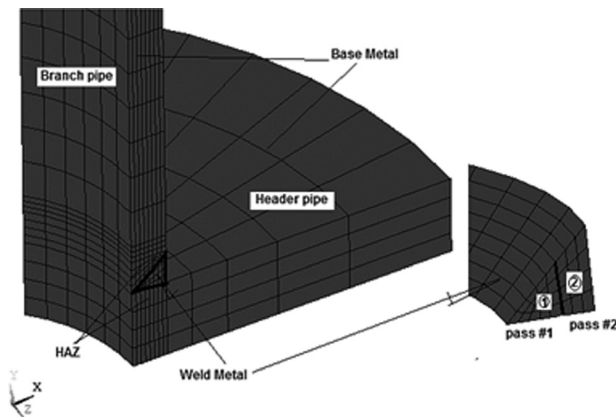


Fig. 11 Finite elements mesh of the tubular model

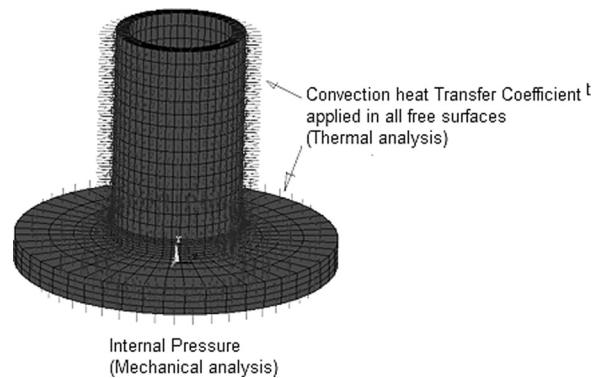


Fig. 12 Boundary conditions

the distance traveled by the welder and the total time measured at each pass, with the aid of two synchronized watches. In addition, control points were established to better establish the average speed of welding. The flow rate and the internal pressure of the fluid (air) were measured to be input data in the definition of the convection coefficient in accordance with expression (7) of Bang et al. [19], and to determine the mechanical stresses due to the internal pressure. The block valve at the end of the flowmeter was used to control the airflow at 400 NL/min and the pressure was adjusted and maintained at 5 kgf/cm 2

$$\frac{h_g D}{k_g} = 0,023 \left(\frac{\rho_g v_g D}{\mu_g} \right)^{0,8} \left(\frac{C_p \rho_g \mu_g}{k_g} \right)^{0,4} \quad (7)$$

This experimental facility allowed evaluating the proposed numerical model with DEHS for circular movement and the methodology to determine the parameters a , b , and c . With the numerical model, it is possible to predict the probability of burn-through, based in elastoplastic stress analysis. Tests with different values of current were performed and the model can predict the failure with amperage of 120 A, as can be seen in Fig. 14. At another

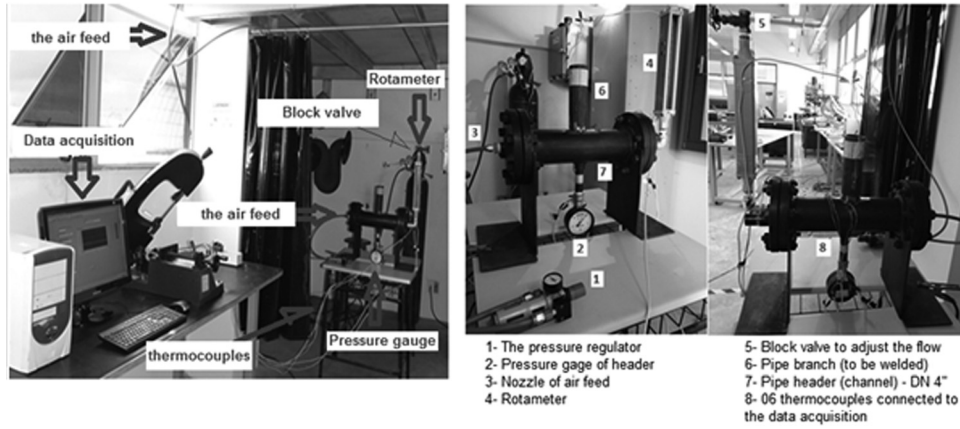


Fig. 13 General view and main components

Table 4 Basic data of the welding process (GTAW)

Efficiency (η)	0,50–0,80 ^a
Travel speed (v)	5–10 cm/min
Voltage (V)	13–18 V
Amperage (I)	80–125 A
Wire diameter/arc length	2,4 mm
Wire specification	ER-70 S
Gas flow	10 L/min

^aSmartt et al. [18]

case, the model predicted that there will not be burn-through with amperage less than 80 A, as can be seen in Fig. 15.

5 Comparing the Proposed Model With Others

References

According to Goldak and Akhlaghi [7], in the last 10 yrs there has been considerable progress in the development of numerical methods for solving this coupled problem with greater speed and

precision methods. It should be remembered that the welding involves numerous passes, each contributes to the mechanical and thermal effects. Lindgren [20] also mentioned that an appropriate model of the heat source can characterize the complex physics of MZ and their interaction in welding. The interaction between the heat transfer, solid mechanics, and metallurgical/material properties is a complex model. And this complexity becomes higher when a fourth component is added to the in-service welding—the process fluid—because there is a direct interaction with others component. Therefore, the authors proposes a comprehensive computational model to simulate and evaluate the feasibility of the hot tapping, as the risks related to welding in pipeline or piping, involving its various aspects and parameters with respect to the welding process (amperage, voltage, travel speed, etc.), material properties, characteristics, and operating conditions of the fluid contained in order to prevent accident during the welding. The proposed model has considered the most current solutions numerical modeling, adopted in various reference works cited, but with the distinction of being applied in the same 3D tubular model and with a new equation for heat source in double ellipsoid considering circular motion as be seen in Table 5 [4,6,21].

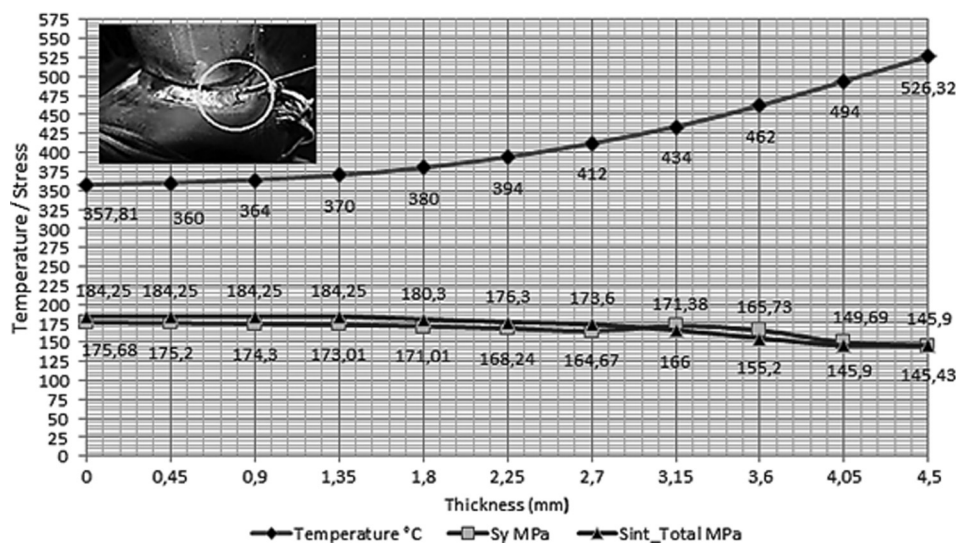


Fig. 14 The proposed numerical model can predict the burn-trough risk with 120 A. The numerical model showed the equivalent stress above the yield stress at 80% of the cross section.

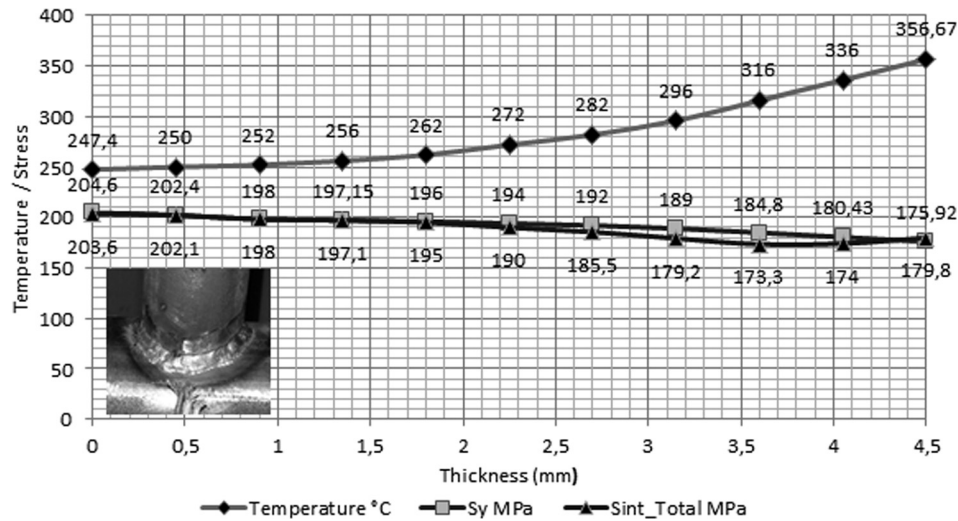


Fig. 15 The proposed numerical model can be predicted which there will not burn-through with 80 A. The numerical model showed the equivalent stress above the yield stress at less than 5% of the cross section.

Table 5 Comparing the proposed model with others models of references in modeling of hot-tapping

From ^b	Year	Geometry			Heat source model			Properties/ microstructure	Solid mechanics		
		2D	3D	Thickness	Movement	Distribution	Weld pass		Thermal stress	Stress due to pressure	Flow of the fluid
Tahami et al.	2010	—	Yes	8,2 to 2,8 mm	Linear	Volume of bead	Multipass	Only changing with temperature	Yes	Yes	Empirical equations
Tahami et al.	2009	Yes	—	15 mm	Linear	Area of bead	Multipass	Only changing with temperature	Yes	Yes	Empirical equations
Sabapathy et al.	2000	—	Yes	3 to 5 mm	Linear	Double ellipsoidal	One pass	Only changing with temperature	No	Yes	Empirical equations
BMI/EWI ^a	1980s	Yes	—	>5 mm	Static	Area of bead	One pass	Only changing with temperature	No	No	Empirical equations
Proposed model	2015	—	Yes	3 to 5 mm	Circular	Double ellipsoidal	Multipass	Only changing with temperature	Yes	Yes	Empirical equations

^aAlthough it was developed in the 1980s, the model BMI/EWI was included for comparison purposes, since it is a model widely used in Brazil.

^bThe characteristics of the proposed model, per this paper, include the most up to solutions, in each dimension or boundary condition for the in-service welding computational model.

6 Conclusions

This paper presented a new equation for heat source in double ellipsoid considering the circular motion, trying to develop a model closer to the physical situation of hot tapping onto pipeline. Second, an analytical methodology for determination of the parameters a , b , and c , and third, the building of an experimental facility to get the temperature field. This facility was used to validate the numerical finite element models based on the proposed mathematical approaching. The new model proposed presents good results when compared with experimental model then it can be used for prediction and risks assessment due to the results had been closed and conservative. Besides, the methodology for determining the parameters a , b , and c will allow automation of the process of simulation numerical due to the good approximating with the adjusted numerical models, and at the future this could avoid the building of experimental facility. However, this mathematical approaching needs to be more stressed, and this will require an assessment of the sensibility of the mathematical model with relation to the variation of all parameters in extreme conditions.

References

- [1] Sabapathy, P. N., Wahab, M. A., and Painter, M. J., 2005, "The Onset of Pipe-wall Failure During 'In-Service' Welding of Gas Pipelines," *J. Mater. Process. Technol.*, **168**(3), pp. 414–422.
- [2] American Petroleum Institute, 2004, "Welding Inspection and Metallurgy," Report No. API 577, Washington, DC.
- [3] American Petroleum Institute, 2003, "Procedures for Welding or Hot Tapping on Equipment Containing," Report No. API 2201, Washington, DC, p. 12.
- [4] Tahami, V.-F., and Asl, M.-H., 2009, "A Two-Dimensional Thermomechanical Analysis of Burn-Through at In-Service Welding of Pressurized Canals," *J. Appl. Sci.*, **9**(4), pp. 615–626.
- [5] Goldak, J. A., Oddy, A. S., and Dorling, D. V., 1993, "Finite Element Analysis of Welding on Fluid Filled," *Pressurised Pipelines*, ASM International, Gatlinburg, TN, pp. 45–50.
- [6] Sabapathy, P. N., Wahab, M. A., and Painter, M. J., 2001, "Numerical Models of In-Service Welding of Gas Pipelines," *J. Mater. Process. Technol.*, **118**(1–3), pp. 14–21.
- [7] Goldak, J. A., and Akhlaghi, M., 2010, *Computational Welding Mechanics*, Springer Books, New York, pp. 32–35.
- [8] Christensen, N., Davies, V., and Gjermundsen, K., 1965, "The Distribution of Temperature in Arc Welding," *Br. Weld. J.*, **12**(2), pp. 54–75.
- [9] Rosenthal, D., 1946, "The Theory of Moving Sources of Heat and Its Application to Metal Treatments," *Trans ASME*, **68**, pp. 849–865.
- [10] Eagar, T. W., and Tsai, N. S., 1983, "Temperature Fields Produced by Traveling Distributed Heat Sources," *Weld. J.*, **62**(12), pp. 346–355.
- [11] Friedman, E., 1975, "Thermo-Mechanical Analysis of the Welding Process Using the Finite Element Method," *ASME J. Pressure Vessel Technol.*, **97**(3), pp. 206–213.
- [12] Krutz, G. W., and Sergerlind, L. J., 1978, "Finite Element Analysis of Welded Structures," *Weld. J. Res. Suppl.*, **57**, pp. 211s–216s.
- [13] American Society of Mechanical Engineers, 2004, *Boiler & Pressure Vessel Code, Section II Part D, Subpart 1 and 2*, ASME, New York, pp. 498–703.
- [14] American Society of Mechanical Engineers, 2010, *Code for Pressure Piping, Process Piping ASME B31.3, Appendix C*, ASME, New York, pp. 209–225.

- [15] Deng, D., and Murokawa, H., 2008, "Finite Element Analysis of Temperature Field, Microstructure and Residual Stress in Multi-Pass Buttwelded 2.25Cr-1Mo Steel Pipes," *Comput. Mater. Sci.*, **43**(4), pp. 681–695.
- [16] ANSYS, 2012, *User's Manual, Mechanical APDL Release 14.5*, ANSYS, Canonsburg, PA.
- [17] Yaghi, A., Hyde, T. H., Becker, A. A., Sun, W., and Williams, J. A., 2006, "Residual Stress Simulation in Thin and Thick-Walled Stainless Steel Pipe Weld Including Pipe Diameter Effects," *Int. J. Pressure Vessels Piping*, **83**, pp. 864–874.
- [18] Smartt, H., Einerson, C. J., and Stewart, J. A., 1985, AWS Annual Meeting, Las Vegas, NV.
- [19] Bang, I. W., Son, Y. P., Oh, K. H., Kim, Y. P., and Kim, W. S., 2002, "Numerical Simulation of Sleeve Repair Welding of In-Service Gas Pipelines," *Weld. J.*, **81**(12), pp. 273-S–282-S.
- [20] Lindgren, L.-E., 2006, "Numerical Modeling of Welding," *Comp. Methods Appl. Mech. Eng.*, **195**, pp. 6710–6736.
- [21] Vakili-Tahami, F., Zehsaz, M., and Saeimi-Sadigh, M., 2010, "Finite Element Analysis of the In-Service Welding of T Joint Pipe Connections," *Eur. J. Sci. Res.* **40**(4), pp. 557–568.